MODELS OF THE SPATIAL VARIATION OF GROUND MOTION FOR SEISMIC ANALYSIS OF STRUCTURES

Erik H. Vanmarcke (I)
Ronald S. Harichandran (II)
Presenting Author: E. Vanmarcke

SUMMARY

New theoretical models that account for spatial as well as temporal variation of earthquake ground motion can be used to generate space-averaged input ground motions for structures with large, rigid foundations as well as correlated input motions for structures with multi-supports. A specific format for ground motion characterization suitable for seismic analysis of spatially extended structures is suggested, and some empirical validation is provided based on statistical analysis of records from the Taiwan seismic array.

INTRODUCTION

To date, it has been common in earthquake engineering to focus attention on the time history of ground acceleration (and its response spectrum) at a given location in space. This is a logical consequence of the fact that much of our knowledge about earthquake ground motion comes from recorded accelerograms, and that engineering attention has traditionally focused on "point" facilities for which it seemed reasonable to ignore "local" spatial variation of ground motion in seismic analysis and design. However, for spatially extended structures such as pipelines and embankments, or structures on widely-separated multiple supports or on large foundation slabs, the spatial variation of ground motion may be just as important as the temporal variation. Empirical strong-motion data from closely spaced arrays of seismographs is now gradually becoming available, and engineers are increasingly directing their attention to the effects of earthquakes on spatially distributed systems.

It is argued herein that analytical models of homogeneous random field theory can be used to represent the space-time character of ground motion in a (locally) homogeneous random medium (say, a particular type of bedrock or a layer of alluvial soil) during the strong phase of an earthquake. In a wide alluvial basin, waves will tend to propagate in all directions, and the resulting random field of ground motions (say, a specified component of horizontal motion) may exhibit an isotropic spatial correlation function. (A more general "ellipsoidal" random field is characterized by a correlation function with ellipsoidal iso-correlation contours.) In addition, it may be appropriate (especially in the near field) to introduce a deterministic phase lag to account for partially predictable wave front propagation.

(I) Professor of Civil Engineering, M.I.T., Cambridge, MA. 02139 USA

(II) Research Assistant, M.I.T., Cambridge, MA. 02139 USA

RANDOM FIELD MODELS

General Second Order Statistics

This section provides the necessary background information on n-dimensional homogeneous space-time processes $X(\underline{u},t)$ which depend on a vector of spatial coordinates $\underline{u}$ and on time t. At a given location in space, $\underline{u} = \underline{u}_o$, the variance with time is represented by the 1-D process $X(\underline{u}_o,t)$, and we denote by $S(\omega)$ the two-sided "point" spectral density function of $X(\underline{u},t)$. Its Fourier transform is the temporal covariance function $B(\tau)$. The assumption of homogeneity in space implies that the statistics of $X(\underline{u},t)$ do not depend on $\underline{u}$. The variance of $X(\underline{u},t)$ is

$$\sigma^2 = \int_{-\infty}^{+\infty} S(\omega)d\omega = B(\tau)\Big|_{\tau=0} \tag{1}$$

The unit-area spectral density function is $s(\omega) = \sigma^{-2}S(\omega)$ and the temporal correlation function is $\rho(\tau) = \sigma^{-2}B(\tau)$. At a given instant, $t = t_o$, the spatial variation is represented by a random field $X(\underline{u},t_o)$ which depends on $(n - 1)$ spatial coordinates. The space-time covariance function is by definition the covariance between two observations at different points $(\underline{u},t)$ and $(\underline{u}',t')$ in the parameter space:

$$B(\underline{u},\underline{u}',t,t') = E[X(\underline{u},t) - m_x)(X(\underline{u}',t') - m_x)]$$

$$= B(\underline{u} - \underline{u}',t - t') = B(\underline{\nu},\tau), \tag{2}$$

where $\underline{\nu}$ is the vector of distance separations ($\nu_1 = u_1 - u_1'$, $\nu_2 = u_2 - u_2'$,...) and τ is the time lag $t - t'$. By converting the time lag τ into a frequency ω, the space-time cross-spectral density function $C(\underline{\nu},\omega)$, is obtained:

$$C(\underline{\nu},\omega) = \frac{1}{2\pi}\int_{-\infty}^{+\infty} B(\underline{\nu},\tau)e^{-i\omega\tau}d\tau \tag{3}$$

If the two (spatial) locations coincide, that is, $\underline{u} = \underline{u}'$ or $\underline{\nu} = \underline{0}$, then

$$B(\underline{0},\tau) \equiv B(\tau) \tag{4}$$

and

$$C(\underline{0},\omega) \equiv S(\omega), \tag{5}$$

Equation 3 then reduces to the one-dimensional Wiener-Khinchine relation between $S(\omega)$ and $B(\tau)$.

Frequency-Dependent Spatial Correlation Function

It is useful to normalize the cross-spectral density function with respect to its value at $\underline{\nu} = \underline{0}$. Define

$$\rho_{\omega}(\underline{\nu}) = \frac{C(\underline{\nu},\omega)}{C(\underline{0},\omega)} = \frac{C(\underline{\nu},\omega)}{S(\omega)} \quad . \tag{6}$$

$\rho_{\omega}(\underline{\nu})$ is the frequency-dependent spatial correlation function (subscripting ω is intended to emphasize the dependence on the distance shift vector $\underline{\nu}$). $\rho_{\omega}(\underline{\nu})$ has the character of a correlation function as it quantifies the degree of spatial correlation associated with individual sinusoidal components of the space-time process $X(\underline{u},t)$. The "composite" spatial correlation function $\rho(\underline{\nu})$ may be expressed as follows (Ref.1):

$$\rho(\underline{\nu}) = \int_{-\infty}^{+\infty} \rho_{\omega}(\underline{\nu}) s(\omega) d\omega, \tag{7}$$

In words, the (composite) correlation function $\rho(\underline{\nu})$ is a weighted combination of frequency-dependent correlation functions $\rho_{\omega}(\underline{\nu})$; the weighting function is simply the unit-area spectral density function $s(\omega)$.

If all but one of the spatial coordinates of the space-time process $X(\underline{u},t)$ is held constant, one obtains a direction-dependent process $X(u_i,t)$, $i = 1,\ldots,n-1$, itself a two-dimensional space-time process. The subscript i identifies the free spatial coordinate. All the relationships stated for n-dimensional space-time processes can also be restated for $X(u_i,t)$.

Quadrant Symmetry

If the homogeneous space-time process $X(\underline{u},t)$ is real, $B(\underline{\nu},\tau)$ will be real, while the partial transform $C(\underline{\nu},\omega)$ will in general be complex. In case $B(\underline{\nu},\tau)$ is quadrant symmetric, all the Fourier transforms will be real (owing to "evenness" with respect to each component of the space-time lag vector). These comments also apply to the frequency-dependent correlation function $\rho_{\omega}(\underline{\nu})$. If the correlation structure of $X(\underline{u},t)$ is quadrant symmetric, $\rho_{\omega}(\underline{\nu})$ will be real; otherwise, it will be complex.

Empirical Study

We report here on a small part of an empirical study of the spatial variation of earthquake motion based on the strong motion part of one component of the accelerograms from an earthquake recorded on January 29, 1981 by the SMART 1 digital seismograph array located in Lotung, Taiwan. These accelerograms have already been studied by others (Ref. 2 and 3), but the processing methods and results presented here differ from those considered before.

The earthquake under study had a 6.9 magnitude and a maximum recorded horizontal acceleration in the north-south direction of 0.24 g. The epicenter was located 30 km from the center of the array at an azimuth of 153.8°, and the focal depth was 11 km. Only the epicentral component (N26°W) is analyzed herein. The layout of the SMART 1 array is shown in Fig. 1. The accelerograms recorded at stations 006, M06, I06, C00, I12, M12, and 012 and at stations 003, M03, I03, C00, I09, M09 and 009 were used in the data processing.

The analysis is based on the assumption that the records constitute limited observations of a space-time random field, the main objective being to estimate the second-order characteristics of this field. Consider two (jointly stationary) random processes $X_j(t) \equiv X(\underline{u}_j,t)$ and $X_k(t) \equiv X(\underline{u}_k,t)$ whose sample functions $x_j(t)$ and $x_k(t)$ extend over the interval $-T/2 \leq t \leq T/2$. The sample cross spectrum of $X_j(t)$ and $X_k(t)$ is (Ref. 4):

$$\overline{S}_{jk}(f) = \int_{-T}^{T} \overline{B}_{jk}(\tau)\, e^{-i2\pi f\tau} d\tau, \tag{8}$$

which is the Fourier Transform of the sample cross covariance function, $\overline{B}_{jk}(\tau)$ and is in general complex. The sample cross spectrum has a high variance and, hence, tends to be very erratic. The associated smoothed cross spectrum involves the use of a weighting function W(f):

$$\hat{S}_{jk}(f) = \int_{-\infty}^{\infty} W(g)\, \overline{S}_{jk}(f)\, dg. \tag{9}$$

By using the property of the convolution integral, the above relation can be shown to be equivalent to

$$\hat{S}_{jk}(f) = \int_{-\infty}^{\infty} w(\tau)\, \overline{B}_{jk}(\tau)\, e^{-i2\pi f\tau} d\tau = \int_{-\infty}^{\infty} \hat{B}(\tau)\, e^{-i2\pi f\tau} d\tau. \tag{10}$$

Here, W(f) and w(τ) form a Fourier Transform pair, and are called the spectral window and the lag window, respectively. The lag window has the properties

$$\begin{aligned} &\text{(i)} \quad w(d) = 1 \\ &\text{(ii)} \quad w(d + \tau) = w(d - \tau) \\ &\text{(iii)} \quad w(\tau) = 0,\ \tau \geq (d + M),\ \tau \leq (d - M),\ (|d| + M) \leq T \end{aligned} \tag{11}$$

Thus, the window is symmetric about the lag d, and has a half-width M.

The significance of these parameters is discussed below.

The autocovariance function and the sample and smoothed autospectra are obtained by setting j = k, and taking d = 0. Since the autocovariance function is symmetric about the origin, the sample and smoothed autospectra are real.

The smoothed coherency spectrum, i.e., an estimate of $\rho_{\nu}(\omega)$, is defined by

$$\hat{\rho}_{jk}(f) = \frac{S_{jk}(f)}{[S_{jj}(f)\, S_{kk}(f)]^{\frac{1}{2}}} \tag{12}$$

and the smoothed phase spectrum by

$$\hat{\phi}_{jk}(f) = \tan^{-1}\left(\frac{\text{Im}\,[S_{jk}(f)]}{\text{Re}\,[S_{jk}(f)]}\right) \quad , \tag{13}$$

where Im [ ] and Re [ ] stand for the imaginary and real parts of the argument. Although the principal value of the phase is in the interval (-90°, 90°], its range can be extended to (-180°, 180°] by identifying the quadrant in the complex plane in which the cross spectral ordinate is located.

The main difference between the estimation of the auto and cross spectra is in the value of the lag-shift parameter d at which the lag window is centered. (For the auto spectrum the value of d is zero). The least bias is introduced into the estimation of the cross spectrum if the lag window is centered such that the aligned phase spectrum $\hat{\phi}'_{jk}(f) = \hat{\phi}_{jk}(f) + 2\pi df$ does not show a linear trend. In most cases where the cross correlation is strong d will correspond to the lag at which the cross covariance function has its peak. The lag-shift parameter, d, indicates the lead/lag relationship, i.e., the gross phase information, of the two processes $X_j(t)$ and $X_k(t)$.

The parameter M controls the degree of smoothing. If M is large the degree of smoothing is low, but the bias in the smoothed spectral estimators is also small. The choice of M is also influenced by the method of post-processing of the estimated spectra (Ref. 5).

Results of the Analysis

The accelerograms from the stations along the two lines from 006 to 012 and from 003 to 009 were processed in a pairwise manner using the method described above.

The lag-shift parameters obtained from the processing, scaled by 100,

are depicted in Figs. 2 and 3. The lead/lag relationship between the accelerograms is indicated by means of the curved arrows. Each arrow indicates the apparent direction of wave propagation while the number on each arrow indicates the value of the lag-shift parameter. Those parameter values that coincide with the peak of the cross covariance function are encircled. It can be seen that a systematic propagation effect is apparent along the direction from 006 to 012, but is not evident in the orthogonal direction. This is not surprising since the direction from 006 to 012, N18°W, is close to the direction from the epicenter to the center of the array, N26°W, along which propagation would be expected to take place. The lag-shift parameters corresponding to the stations on the line from 006 to 012 are plotted against the separation between stations in Fig. 4. By fitting a straight line, by eye, the gross velocity of propagation is estimated to be about 3600 m/sec. This implies that the waves propagate principally through the bedrock and then turn upward into the soft soil at the site.

It can be seen in Figs. 2 and 3 that the lag-shift parameters have an approximate closure property. That is, for a triplet i, j, k of stations lying on a straight line, we have $d_{ik} \simeq d_{ij} + d_{jk}$, algebraically. This property was used to obtain a consistent set of aligned phases: $\hat{\phi}'(f) = \hat{\phi}_{jk}(f) + 2\pi d_{jk} f$. An alternative, physically appealing interpretation is that these are the phases of the aligned accelerograms, $y_j(t)$, obtained from the original accelerograms, $x_j(t)$, through

$$y_1(t) = x_1(t) \; ; \quad y_j(t) = x_j(t - d_{1j}) \quad , \quad j = 2,3.... \tag{14}$$

Thus, the accelerograms obtained from the stations lying along a straight line are aligned relative to one of them. Of course, this alignment alters only the phases and not the absolute values of coherency. Preliminary analyses (Ref. 5) showed that the absolute values of coherency and the aligned phases were functions only of the separation, ν, between each pair of stations and the frequency, f, i.e., $\hat{\rho}_{jk}(f)$ may be written as $\hat{\rho}_{\nu_I}(f)$, where ν_I is the separation between stations j and k. Furthermore, the absolute values of coherency and aligned phases corresponding to pairs of stations along the two lines from 006 to 012 and from 003 to 009 were very similar. Thus, the aligned accelerograms may be considered as samples from an <u>isotropic</u> random field.

Since the lag window used in the processing was wide, the resulting coherency spectra of the aligned accelerograms were quite erratic. For the purposes of viewing and interpretation, these were further smoothed according to

$$\tilde{\rho}_{\nu}(f) = \sum_{i=1}^{m} \sum_{j=1}^{n} \hat{\rho}_{\nu_I}(f_j) \, K\left(\frac{\nu - \nu_I}{\Delta\nu}\right) K\left(\frac{f - f_j}{\Delta f}\right) \Bigg/ \sum_{i=1}^{m} \sum_{j=1}^{n} K\left(\frac{\nu - \nu_I}{\Delta\nu}\right) K\left(\frac{f - f_j}{\Delta f}\right) \tag{15}$$

where $K(x) = e^{-x^2/2}$. The parameters $\Delta\nu$ and Δf, which control the degree of smoothing, were chosen to be 40 m and 0.66 Hz, respectively. The absolute value and phase components of $\rho_{\nu}(f)$ are shown in Figs. 5, 6 and 7.

It can be seen that the absolute value of coherency decays with increasing separation and frequency. For the low frequencies from 0 to about 3 Hz the absolute value of coherency is approximately constant for a given separation. There appears to be a corner frequency between 3 and 4 Hz after which the coherency decays more rapidly. It is clear that the aligned phases are approximately zero for the separations and frequencies of interest. This suggests that the propagation (phase) and correlation (absolute value of coherency) parts can be separated, at least approximately, by utilizing the lag-shift parameters. This decoupling and the resulting isotropy, which are achieved through the alignment procedure, are very desirable properties both from conceptual and modelling points of view.

References

1. Vanmarcke, E.H., "Random Fields: Analysis and Synthesis, The MIT Press, Cambridge, Mass. and London, England, 1983.
2. Bolt, B.A., et. al., "Preliminary Report on the SMART 1 Strong Motion Array in Taiwan", EERC Rept. UCB/EERC-82/13, UC,Berkeley, CA., Aug., 1982.
3. Loh, C.H., Ang, A. H-S, and Wen, Y.K., "Spatial Correlation Study of Strong Motion Array Data with Application to Lifeline Earthquake Engineering", U Illinois Dept. of C.E., Rept. UILU-ENG-83-2002, March, 1983.
4. Jenkins, G.M., and Watts, D.G., Spectral Analysis and Its Applications, Holden-Day, 1969.
5. Harichandran, R.S., "Spatial Variation of Earthquake Motion", Ph. D. Thesis, M.I.T., June, 1984 (expected date).

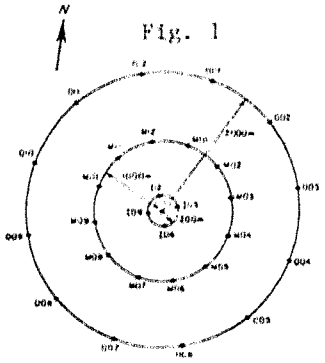

Fig. 1

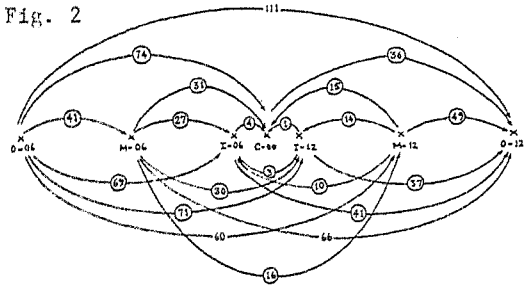

Fig. 2

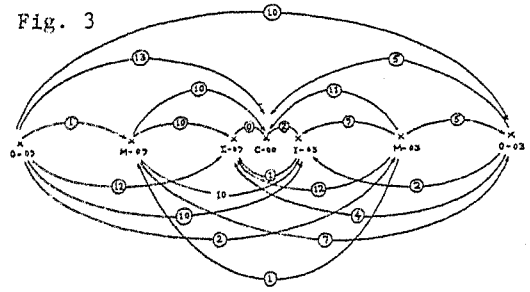

Fig. 3

Fig. 1: The SMART 1 array

Fig. 2: Lag-shift parameters - 006 to 012

Fig. 3: Lag-shift parameters - 003 to 009

This research was funded by NSF under Grant No. CEE-8211021

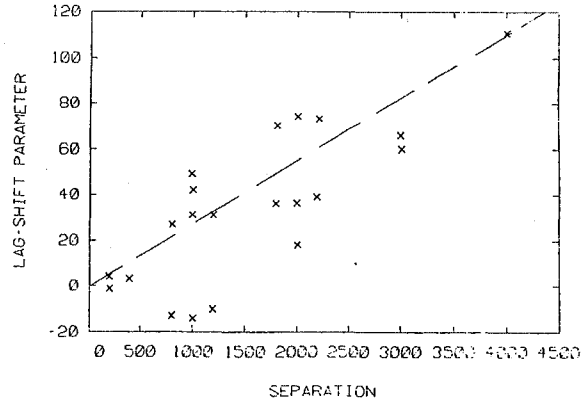

Fig. 4 Lag-shift parameter vs. separation

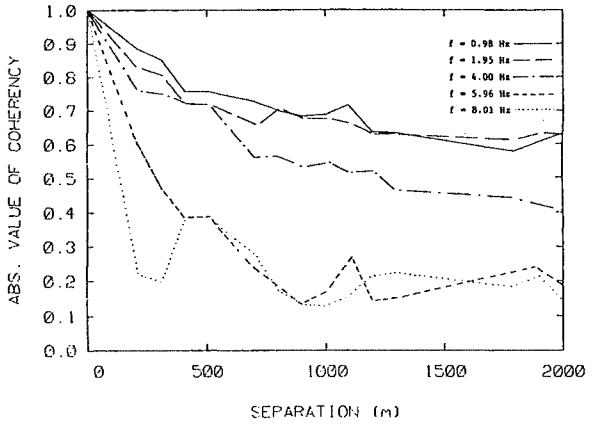

Fig. 6 Abs. value of coherency vs. separation

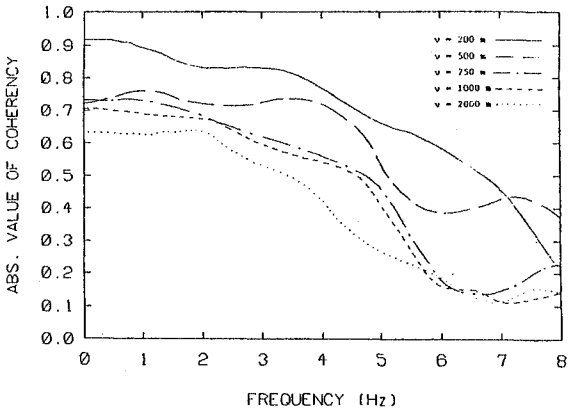

Fig. 5 Abs. value of coherency vs. frequency

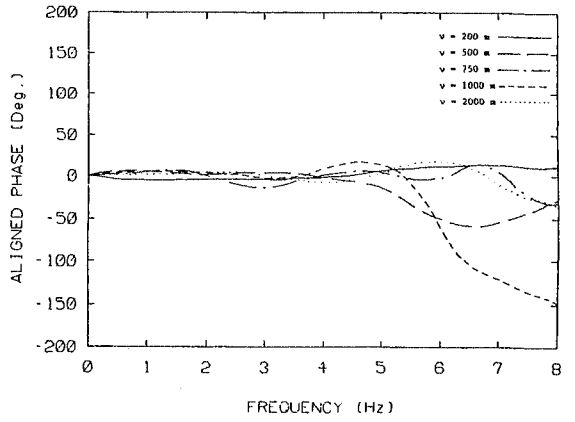

Fig. 7 Aligned phase vs. frequency